Realistic Simulations of White Dwarf Tidal Disruption Events

Sinead Humphrey*

Department of Physics, University of Wisconsin-Milwaukee
Milwaukee, WI, United States of America

Abstract

White dwarfs that pass within the tidal radius of low and intermediate mass black holes can be torn apart by intense tidal forces. This event could ignite thermonuclear burning in the white dwarf which might lead to a distinct observational signal. We present the preliminary findings from 13 numerical simulations of white dwarf tidal disruption events performed using the 3D moving-mesh hydrodynamic code, MANGA, with a new nuclear burning module.

1. Introduction

White dwarfs (WDs) are the extremely dense remnant cores of stars that have exhausted their fuel. They no longer undergo nuclear fusion and are instead supported against collapse by electron degeneracy pressure. The composition of the WD depends on its mass: WDs with masses around $0.4\,\mathrm{M}_\odot$ are composed of mostly helium, $0.5-1\,\mathrm{M}_\odot$ WDs are composed of carbon and oxygen, and WDs with masses above $1.0\,\mathrm{M}_\odot$ are composed of mostly oxygen and neon.

A white dwarf tidal disruption event (WD TDE) occurs when a WD enters the tidal radius of a black hole (BH) and is torn apart by tidal forces.

Following the formalism of Guillochon and Ramirez-Ruiz (2013), there are a few parameters we use to define a WD TDE. The first is the tidal radius, r_T, given by

$$r_\mathrm{T} = \left(\frac{M_\mathrm{BH}}{M_*}\right)^{1/3} R_*, \tag{1}$$

where M_BH is the mass of the black hole, M_* is the mass of the star, and R_* is the radius of the star.

We then define the impact parameter β to be

$$\beta \equiv \frac{r_\mathrm{T}}{r_\mathrm{p}}, \tag{2}$$

where r_p is the periaspe of the orbit assuming Keplerian dynamics. This β characterizes the strength of the event with a higher β corresponding to a deeper penetration of the WD into the tidal radius of the BH.

Because of how the tidal radius of the BH scales with its mass, only stellar mass to intermediate mass black holes (IMBHs) are capable of disrupting a WD (Maguire et al., 2020). IMBHs have yet to be directly detected; this makes WD TDEs particularly interesting as they would serve as probes of the population of IMBHs. Additionally, during disruption, the WD becomes compressed which may lead to ignition of nuclear burning (Maguire et al., 2020). Thermonuclear reactions could give the WD TDE a unique electromagnetic signature that would appear as a transient event and would be best detected in time domain sky surveys such as the Legacy Survey of Space and Time (LSST) at the Vera Rubin Observatory.

*This author is supported by NASA under Award No. RFP23_8-0 through the Wisconsin Space Grant Consortium Graduate and Professional Research Fellowship.

Complex systems like WD TDEs cannot be fully understood through analytical methods, so we instead turn to high-resolution, physically realistic 3D simulations. There are two main methodologies for hydrodynamic simulations: Lagrangian smoothed-particle hydrodynamic (SPH) codes and Eulerian grid codes. SPH uses a mesh free method that models a fluid as a collection of particles. This method maintains conserved quantities but has poor shock resolution due to smoothing. Eulerian grid codes, on the other hand, divide a fluid onto a grid and calculate flux through adjacent boundaries. Eulerian codes are good at capturing discontinuities such as shocks, but they do not obey conservation laws well.

Arbitrary Lagragian-Eulerian (ALE) or "moving-mesh" schemes offer a third option where a mesh is generated from points that move with the fluid. This method combines the best features of SPH and Eulerian methods i.e. it captures shocks well while maintaining conserved quantities.

2. Methodology

We use the moving-mesh hydrodynamic code, MANGA (Chang et al., 2017; Prust and Chang, 2019; Chang et al., 2020; Chang and Etienne, 2020), to simulate WD TDEs. We recently developed a nuclear burning module in MANGA which uses the nuclear reaction network, approx21 (Timmes et al., 2000), that is implemented in MESA (Paxton et al., 2011, 2013, 2015, 2018; Paxton, 2019). A detailed discussion of the nuclear burning module can be found in Humphrey (2023).

We have also included the nuclear burning limiter described in Kushnir et al. (2013). This limits the energy generation rate to $\dot{e} < fec_s/\Delta x$, where e is the internal energy of the cell, c_s is the sound speed of the cell, Δx is the size of the cell, and $f = 0.1$ is an arbitrary constant. This limiter is intended to prevent the nuclear energy generation rate from changing the local internal energy too rapidly.

3. Results

We present the results of 13 WD TDEs simulated in MANGA. All simulations include an atmosphere with density $\rho = 0.01\,\mathrm{g\,cm^{-3}}$ and use a $1000\,\mathrm{M}_\odot$ BH modeled as a softened dark matter particle.

Figure 1 shows four frames, each 1.5 seconds apart, of the projected density of a WD TDE simulated in MANGA. This simulation corresponds to run 2 on Table 1. It uses 200K particles for the WD, $\beta = 5$, and a $0.6\,\mathrm{M}_\odot$ CO WD. Moving from frame 1 in the upper left to frame 4 in the lower right, we see that as the WD swings around the BH in the center of each frame, it becomes completely disrupted.

Table 1 gives a summary of results of a small parameter study varying the impact parameter, β, and the mass of the WD (M_{WD}). Because the composition of the WD is correlated to its mass, the $0.6\,\mathrm{M}_\odot$ and $0.9\,\mathrm{M}_\odot$ WDs are carbon-oxygen (CO), and the $1.1\,\mathrm{M}_\odot$ WD is oxygen-neon (ONe). We look at three different results from each simulation: the energy generated from nuclear burning (E_{burn}) calculated from the binding energies of the isotopes, the mass burned (M_{burned}), and the total mass of iron group elements created (Fe).

Table 1 also includes a small resolution study of one system using a $0.6\,\mathrm{M}_\odot$ CO WD and $\beta = 5$. For this, we varied the number of mesh generating particles used to make the WD. Because the burning limiter depends on the size of the cell, we chose to turn off the burning limiter for this study to better directly compare between resolutions.

Figure 2 shows the results of the resolution study and corresponds to runs 11, 12, and 13 in Table 1. Each simulation uses a $0.6\,\mathrm{M}_\odot$ CO WD and $\beta = 5$. We plot remaining mass of the original elements of WD as well as the masses of the silicon and nickel formed right after nuclear burning has stopped as a function of N, the number of mesh-generating points used for the WD.

4. Discussion

The production of nickel is particularly important for understanding the observability of WD TDEs as radioactive nickel decay results in significant emission in the optical. Understanding the extent of the nuclear burning and nickel production that might occur in WD TDEs will better help us predict what their observational signals may look like.

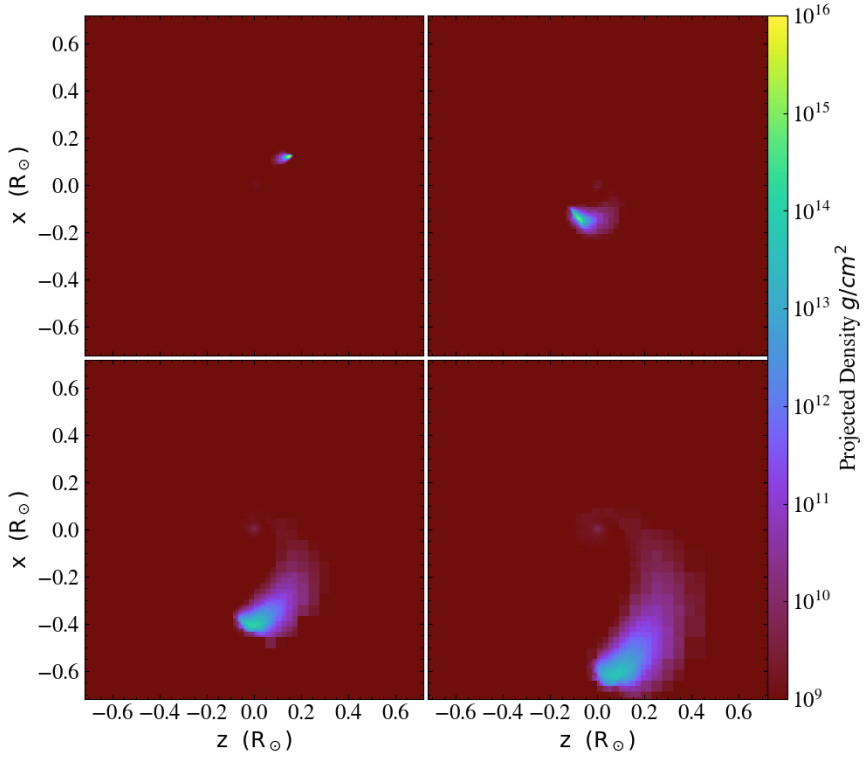

Figure 1: The projected density of a WD TDE simulated in MANGA. 200,000 mesh-generating points were used for the WD. We used a black hole with a mass of $10^3\,\mathrm{M}_\odot$, a WD with a mass of $0.6\,\mathrm{M}_\odot$, and $\beta = 5$. Each frame is 1.5 seconds apart.

Run	β	N	$M_{\mathrm{WD}}(\mathrm{M}_\odot)$	$log(E_{\mathrm{burn}})$	M_{burned} ($\mathrm{M}_\odot$)	Fe ($\mathrm{M}_\odot$)
1	2	200k	0.6	-	0	0
2	5	200k	0.6	50.29	0.153	0.005
3	6	200k	0.6	50.61	0.314	0.040
4	7	200k	0.6	50.76	0.428	0.121
5	8	200k	0.6	50.84	0.491	0.220
6	10	200k	0.6	50.91	0.561	0.383
7	2	200k	0.9	51.01	0.767	0.362
8	5	200k	0.9	51.07	0.835	0.620
9	1	200k	1.1	51.15	1.1	1.088
10	2	200k	1.1	51.16	1.1	1.094
11†	5	200k	0.6	50.80	0.473	0.106
12†	5	1M	0.6	50.76	0.424	0.126
13†	5	2M	0.6	50.45	0.212	0.023

Table 1: A summary of simulations of WD TDEs simulated in MANGA. All simulations use a BH mass of $1000\,\mathrm{M}_\odot$. N is the number mesh-generating points used for the WD. E_{burn} is the energy generated from nuclear burning in ergs. "Fe" gives the total mass of iron group elements. Simulations marked with a † are run without a burning limiter.

4.1. Impact Parameter The impact parameter, β, appears to have a significant effect on the amount of nuclear burning that occurs. Spaulding and Chang (2021) found that, in the case of stellar TDEs, systems with higher β values had earlier fallback of stellar gas onto the BH. They also found that the energy spread of the gas scaled as $\beta^{1/2}$ for β values from 2 to 9 and asymptotes for $\beta \gtrsim 10$. This energy spread might appear as different compression ratios which may affect the amount of nuclear burning in WD TDEs. In Table 1 we see a trend of higher β interactions undergoing more nuclear burning. This can be seen in runs 1 through 6 where we observe increasing values of $E_{\rm burn}$, $M_{\rm burned}$, and the mass of iron group elements created as β increases.

Additionally, Rosswog et al. (2009) found that less massive WDs require a higher β to ignite nuclear burning, which does appear in our study. Looking at runs 1 and 7, which both have $\beta = 2$ and use an initial CO WD, we see that the $0.6\,\mathrm{M}_\odot$ WD undergoes no nuclear burning whereas the $0.9\,\mathrm{M}_\odot$ WD undergoes significant nuclear burning converting about 40% of its mass into iron group elements. Further we can compare to run 10 with a $1.1\,\mathrm{M}_\odot$ ONe WD and $\beta = 2$. This system undergoes even more nuclear burning, with nearly all of the WD's mass being converted into iron group elements. However this WD has a different initial composition and so is not a direct comparison to the other two systems.

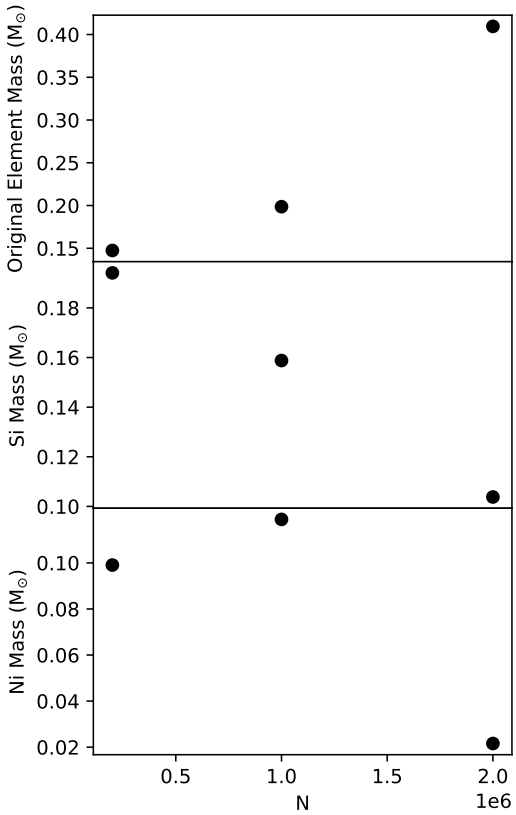

Figure 2: A plot of the remaining original element mass as well as the mass of silicon and nickel created during nuclear burning as a function of N, the number of mesh-generating points used for the WD. Values are taken from a time right after nuclear burning has ceased.

4.2. Resolution In Figure 2, we can see that as resolution increases so does the original element mass i.e. the unburnt material. Further, as resolution increases the mass of silicon created decreases. Curiously, the mass of nickel created increases between $\mathrm{N} = 200\mathrm{k}$ and $\mathrm{N} = 1\mathrm{M}$ but then decreases when $\mathrm{N} = 2\mathrm{M}$. Tanikawa et al. (2017) performed high resolution 3D SPH simulations of WD TDEs and they observed that nuclear reactions reduce with increased number of SPH particles. They argue that nuclear reactions occur at low resolution in SPH simulations due to spurious heating. Further investigation, however, is needed to understand the resolution requirements for WD TDE simulations on a moving mesh.

Acknowledgments

We thank Philip Chang for helpful discussion and advice. This work was supported by NASA under Award No. RFP23_8-0 through the Wisconsin Space Grant Consortium Graduate and Professional Research Fellowship. We use the YT python package for the analysis of the data and generation of plots in this work (Turk et al., 2011). Computational work was done on the University of Wisconsin-Milwaukee High Performance Computing cluster, Mortimer.

References

P. Chang and Z. B. Etienne. General relativistic hydrodynamics on a moving-mesh i: static space–times. *MNRAS*, 496 (1):206–214, jun 2020. doi: 10.1093/mnras/staa1532.

P. Chang, J. Wadsley, and T. R. Quinn. A moving-mesh hydrodynamic solver for ChaNGa. *MNRAS*, 471:3577–3589, Nov. 2017. doi: 10.1093/mnras/stx1809.

P. Chang, S. W. Davis, and Y.-F. Jiang. Time-dependent radiation hydrodynamics on a moving mesh. *MNRAS*, 493 (4):5397–5407, Apr. 2020. doi: 10.1093/mnras/staa573.

J. Guillochon and E. Ramirez-Ruiz. Hydrodynamical Simulations to Determine the Feeding Rate of Black Holes by the Tidal Disruption of Stars: The Importance of the Impact Parameter and Stellar Structure. *ApJ*, 767(1):25, Apr. 2013. doi: 10.1088/0004-637X/767/1/25.

S. Humphrey. Numerical simulations of white dwarf tidal disruption events. *Proceedings of the 32nd Annual Wisconsin Space Conference*, 2023. doi: https://doi.org/10.17307/wsc.v1i1.371.

D. Kushnir, B. Katz, S. Dong, E. Livne, and R. Fernández. Head-on Collisions of White Dwarfs in Triple Systems Could Explain Type Ia Supernovae. *ApJL*, 778(2):L37, Dec. 2013. doi: 10.1088/2041-8205/778/2/L37.

K. Maguire, M. Eracleous, P. G. Jonker, M. MacLeod, and S. Rosswog. Tidal Disruptions of White Dwarfs: Theoretical Models and Observational Prospects. *SSR*, 216(3):39, Mar. 2020. doi: 10.1007/s11214-020-00661-2.

B. Paxton. Modules for Experiments in Stellar Astrophysics (MESA). Zenodo, Sept. 2019.

B. Paxton, L. Bildsten, A. Dotter, F. Herwig, P. Lesaffre, and F. Timmes. Modules for Experiments in Stellar Astrophysics (MESA). *ApJS*, 192:3, Jan. 2011. doi: 10.1088/0067-0049/192/1/3.

B. Paxton, M. Cantiello, P. Arras, L. Bildsten, E. F. Brown, A. Dotter, C. Mankovich, M. H. Montgomery, D. Stello, F. X. Timmes, and R. Townsend. Modules for Experiments in Stellar Astrophysics (MESA): Planets, Oscillations, Rotation, and Massive Stars. *ApJS*, 208:4, Sept. 2013. doi: 10.1088/0067-0049/208/1/4.

B. Paxton, P. Marchant, J. Schwab, E. B. Bauer, L. Bildsten, M. Cantiello, L. Dessart, R. Farmer, H. Hu, N. Langer, R. H. D. Townsend, D. M. Townsley, and F. X. Timmes. Modules for Experiments in Stellar Astrophysics (MESA): Binaries, Pulsations, and Explosions. *ApJS*, 220:15, Sept. 2015. doi: 10.1088/0067-0049/220/1/15.

B. Paxton, J. Schwab, E. B. Bauer, L. Bildsten, S. Blinnikov, P. Duffell, R. Farmer, J. A. Goldberg, P. Marchant, E. Sorokina, A. Thoul, R. H. D. Townsend, and F. X. Timmes. Modules for Experiments in Stellar Astrophysics (MESA): Convective Boundaries, Element Diffusion, and Massive Star Explosions. *ApJS*, 234(2):34, Feb. 2018. doi: 10.3847/1538-4365/aaa5a8.

L. J. Prust and P. Chang. Common envelope evolution on a moving mesh. *MNRAS*, 486(4):5809–5818, July 2019. doi: 10.1093/mnras/stz1219.

S. Rosswog, E. Ramirez-Ruiz, and W. R. Hix. Tidal Disruption and Ignition of White Dwarfs by Moderately Massive Black Holes. *ApJ*, 695(1):404–419, Apr. 2009. doi: 10.1088/0004-637X/695/1/404.

A. Spaulding and P. Chang. The effect of impact parameter on tidal disruption events. *mnras*, 501(2):1748–1754, Feb. 2021. doi: 10.1093/mnras/staa3627.

A. Tanikawa, Y. Sato, K. Nomoto, K. Maeda, N. Nakasato, and I. Hachisu. Does Explosive Nuclear Burning Occur in Tidal Disruption Events of White Dwarfs by Intermediate-mass Black Holes? *apj*, 839(2):81, Apr. 2017. doi: 10.3847/1538-4357/aa697d.

F. X. Timmes, R. D. Hoffman, and S. E. Woosley. An Inexpensive Nuclear Energy Generation Network for Stellar Hydrodynamics. *ApJS*, 129(1):377–398, July 2000. doi: 10.1086/313407.

M. J. Turk, B. D. Smith, J. S. Oishi, S. Skory, S. W. Skillman, T. Abel, and M. L. Norman. yt: A Multi-code Analysis Toolkit for Astrophysical Simulation Data. *ApJS*, 192(1):9, Jan. 2011. doi: 10.1088/0067-0049/192/1/9.